Asia-Pac. J. Atmos. Sci., 50(2), 221-227, 2014
DOI:10.1007/s13143-014-0010-0

Characteristics of Velocity Ambiguity for CINRAD-SA Doppler Weather Radars

Zhigang Chu[1], Yan Yin[1], and Songshan Gu[2]

[1]*Key Laboratory of Meteorological Disaster of Ministry of Education, Nanjing University of Information Science & Technology, Nanjing, China*
[2]*Key Laboratory for Aerosol-Cloud-Precipitation of China Meteorological Administration, Nanjing University of Information Science & Technology, Nanjing, China*

(Manuscript received 2 February 2013; accepted 20 August 2013)

Abstract: The velocity ambiguity in Doppler weather radars has inhibited the application of wind field data for long time. One effective solution is software-based velocity dealiasing algorithm. In this paper, in order to better design, optimize and validate velocity dealiasing algorithms for CINRAD-SA, data from operational radars were used to statistically characterize velocity ambiguity. The analyzed characteristic parameters included occurrence rate, and inter-station, inter-type, temporal, and spatial distributions. The results show that 14.9% of cloud-rain files and 0.3% of clear-air files from CINRAD-SA radars are ambiguous. It is also found that echoes of weak convections have the highest occurrence rate of velocity ambiguity than any other cloud types, and the probability of ambiguity is higher in winter than in summer. A detailed inspection of the occurrence of ambiguity in various cases indicates that ambiguous points usually occur in areas with an elevation angle of 6.0°, an azimuth of 70° or 250°, radial distance of 50-60 km, and height of 5-6 km, and that 99.4% of ambiguous points are in the 1st-folding interval. Suggestions for performing dealiasing at different locations and different time points are provided.

key words: Weather radar, quality control, radial velocity, velocity ambiguity, velocity dealiasing, statistical characterization

1. Introduction

Radial velocity field is one type of data observed by Doppler weather radars and it is widely used in data assimilation, wind field retrieval, nowcasting, and disaster monitoring. Its application has a significant importance in modern weather forecast. However, velocity ambiguity will severely impact the quality of radial velocity, and may result in wrong data assimilation and wrong wind field retrieval. For instance, when velocity azimuth display (VAD; Browning *et al*., 1968) is used in wind field retrieval, relative root-mean-square errors can reach 50% even if 3% of a full volume scan of radial wind data is ambiguous (Gao *et al*., 2004).

Doppler weather radars obtain the radial velocity of a target by measuring the interpulse phase difference. The velocity measurement ranges within $(-V_{\max}, +V_{\max})$, where $V_{\max}$ is called Nyquist velocity and is expressed as:

$$V_{\max} = \frac{\lambda(PRF)}{4}, \tag{1}$$

where λ is radar wavelength and PRF is pulse repetitive frequency. The relationship between the true velocity (V_T) and the measured velocity (V_r) is expressed as:

$$V_T = V_r \pm 2nV_{\max},\ n = 0、\pm 1、\pm 2、..., \tag{2}$$

where n is called Nyquist number. If true velocity is smaller than Nyquist velocity, then Nyquist number is 0, so V_r is unambiguous. If true velocity is larger than Nyquist velocity, then Nyquist Number is not 0, so V_r is ambiguous. The process of solving n is called velocity dealiasing.

The objective of velocity dealiasing is to correct velocity ambiguity in operational radar data. Velocity dealiasing can be realized through hardware- or software-based algorithms. One hardware-based algorithm is the staggered-PRT (staggered Pulse Repetition Time; Doviak *et al*., 1993), which can amplify $V_{\max}$ many times. However, these methods have some shortcomings, such as non-uniform sampling (He *et al*., 2011) and inability of radar system updating. Besides, even if the staggered-PRT can be used, velocity ambiguity still occurs when V_T is large, like in tropical storms or tornados. Therefore software-based methods (velocity dealiasing algorithms) have become a hotspot in the past three decades.

Velocity dealiasing algorithms include interactive and automatic ones. Interactive algorithms depend on expert knowledge and computer technology. Firstly, the experts manually identify the velocity ambiguity points or areas, and then correct them based on the principle that velocity fields are continuous. Interactive methods are precise but arduous, and thus are inconvenient in processing large dataset, especially in real-time operations. Therefore these methods (e.g., Hennington, 1981; Wei *et al*., 2009) are used only as supplement to automatic methods.

Automatic methods can dealiase velocities without human interference, but are less precise than interactive methods. Automatic methods include 1D radial (Ray *et al*., 1977; Bargen *et al*., 1980; Boren *et al*., 1986) or azimuthal methods (Yamada *et al*., 1999; Gong *et al*., 2003; Haase *et al*., 2004; Xu *et al*., 2011), 2D radial and azimuthal methods (Merritt, 1984; Bergen *et al*., 1988; Eilts *et al*., 1990; Jing *et al*., 1993; Zhang *et al*.,

Corresponding Author: Yan YIN, Nanjing University of Information Science & Technology, No. 219 Ningliu Road, Nanjing 210044, China.
E-mail: yinyan@nuist.edu.cn

2006; Witt *et al*., 2009; Li *et al*., 2010), and 4D radial, azimuthal, elevation and temporal methods (James *et al*., 2001). These methods all suppose that velocity field is temporally and spatially continuous, and identify and correct ambiguity by checking abrupt changes.

However, due to impacts from noise, missing data and wind shear, the condition for continuous velocity field usually do not hold, so dealiasing algorithms all produce errors to some degree. How to optimize dealiasing algorithms based on the existing methods and how to improve performance in operational environment are key issues in the field of radar meteorology.

Though velocity dealiasing has been investigated for many years, most of the previous studies focused on methods rather than the characteristics of velocity ambiguity. As a result, the characteristics of velocity ambiguity in operational radars are still unknown. In long-term radar data, for instance, how often ambiguity occurs? Which types of echoes have the highest rate of ambiguity? Which areas in 3D space contain the fewest ambiguous points?

The characteristics of velocity ambiguity can provide some reference for design, optimization and validation of velocity dealiasing algorithms, mainly reflected in the following three aspects.

First, the proportion of ambiguous data in operational radars decides the type of velocity dealiasing algorithms to be used. If the proportion is low, interactive algorithms are suitable as they have high precision. Otherwise automatic algorithms should be used.

Second, the spatial characteristics of velocity ambiguity can be used to solve the initial problem of dealiasing algorithms. Due to the lack of reliable reference information, all algorithms are weakest at processing initial areas or initial radials. Ambiguous data present in the initial area or initial radial would result in numerous errors. Usually, these errors will be spread to impact more data. To solve this problem, Zhang *et al*. (2006) proposed to search the weakest wind region and identify areas with small radial velocity as the initial position. This approach is okay in average sense but not satisfactory for all cases. It will fail with the interference by ground clutter noise and the ambiguous area with small radial velocity in stratus. Therefore, the above problem can be statistically solved by characterizing the spatial distribution of ambiguity, and then finding the elevation angle, azimuth and radial distance with the lowest occurrence rate of ambiguity as the initial position.

Third, the echo types and the temporary distribution of velocity ambiguity can provide reference for algorithm validation. The existing velocity dealiasing algorithms all adopt strong convections for validation, such as tornado, hailstorms, and gust fronts in Eilts *et al*. (1990), tornado, typhoon and hurricane in Zhang *et al*. (2006), and typhoon in He *et al*. (2011). Because the ambiguity in stratus and weak convections was ignored, these validation results cannot reflect the performance of dealiasing algorithms in processing operational radar data. If representative datasets were used to validate the algorithms according to the echo types and the temporary distribution of velocity ambiguity, the overall performances of the algorithms can be evaluated.

The performance of velocity ambiguity is diversified. The occurrence rates and characteristics of velocity ambiguity are distinct among radars, heights, regions, or types of echoes. For instance, radars with large V_{max} have a low occurrence rate of ambiguity; whereas high-altitude echoes have a high occurrence rate of ambiguity. In this paper, three-year full operational data of four CINRAD-SA radars (a S-band Doppler weather radar in China New Generation Weather Radar Network) were used (Section 2); Characteristics of velocity ambiguity were analyzed, including occurrence rate, and inter-station, inter-type, temporal, and spatial distributions (Section 3).

2. Radar data and methods

CINRAD (China New Generation Radar) Network is an observation network composed of 158 Doppler weather radars. CINRAD-SA is an S-band radar and is located along coastal areas, Yangtze and Yellow Rivers in China.

CINRAD-SA has similar performance as WSR-88D used in USA NEXRAD (Next-Generation Radar) network, and its parameters are listed in Table 1. CINRAD-SA has a wavelength around 10 cm, and its velocity field has a radial resolution of 250 m and an azimuthal resolution of 1°. Volume Coverage Pattern 21 (VCP21) scan mode was selected, including 9 elevation angles as 0.5, 1.5, 2.4, 3.4, 4.3, 6.0, 9.9, 14.6, and 19.5°. When elevation angle $\leqq 6°$, $V_{max} \approx 27$ m s^{-1}; when elevation angle $> 6°$, $V_{max} \approx 31$ m s^{-1}. As an operational radar, CINRAD-SA produces a volume file every 6 minutes. It runs 24 hours from May to September and 6 hours in other months, so one radar produces about 50,000 volume files on average per year.

In this paper, data from Fuzhou, Wenzhou, Hefei and Wuhan radars between 2008 and 2010 were selected for analyzing the characteristics of velocity ambiguity. Fuzhou and Wenzhou are seashore radars, Hefei and Wuhan are inland radars (Fig. 1). The four radars have been operating for nearly ten years with good performance.

A total of 614,597 volume files were collected, each with 9 tilts. First, the volume files were divided into cloud-rain files

Table 1. Parameters of CINRAD-SA in China.

Parameter	Value
Wavelength (cm)	~10
Radial Resolution (m)	250
Azimuth Resolution (°)	~1
Scan Mode	Volume Scan (Volume Coverage Pattern 21)
Elevation Angles (°)	0.5, 1.5, 2.4, 3.4, 4.3, 6.0, 9.9, 14.6, 19.5
V_{max}(m s^{-1})	~27 (Elevation Angle < 6.0°) ~31 (Elevation Angle ≧ 6.0°)
Volume File Interval (minute)	~6

Fig. 1. Locations of the selected radar stations.

and clear-air files based on the presence of cloud-rain echoes. If any tilt contains cloud-rain echoes (echoes from cloud or rain droplets), this volume file is classified as cloud-rain, otherwise it is a clear-air file. After this classification, there were 279,283 (45.4%) cloud-rain files and 335,314 (54.6%) clear-air files. Both the cloud-rain and clear-air files were then divided into ambiguous and unambiguous files, based on the presence of ambiguous areas. If any tilt contains ambiguous areas, this file is considered as ambiguous, otherwise it is unambiguous. Based on this classification, 41,687 cloud-rain files and 1,162 clear-air files are ambiguous (accounts for 7.0% of all the files) and 237,596 cloud-rain files and 334,152 clear-air files are unambiguous.

3. Characterization of velocity ambiguity

Figure 2 shows the composition of all the selected volume scan files. About 54.6% of CINRAD-SA data are clear-air files without cloud or rain echoes. It can be seen that about 14.9% of cloud-rain files are ambiguous. This proportion is very high, because under the current scan mode, CINRAD-SA could produce 1.5 ambiguous cloud-rain files per hour in rainy weather. Therefore, dealiasing is necessary for CINRAD-SA cloud-rain files. Due to the high proportion of ambiguous files, only automatic algorithms are suitable, since interactive methods cannot meet the timely processing requirements. About 0.3% of clear-air files are ambiguous. Most clear-air echoes appear in the atmospheric boundary layer, where wind velocity is lower than that at high altitudes and will not exceed the measurement range of CINRAD-SA, so ambiguous clear-air files are relatively few. Besides, clear air files are rarely involved in the application of velocity data, so they can be ignored in dealiasing algorithms. Therefore, clear-air files are not included in the following sections, so all ambiguous files refer to ambiguous cloud-rain files, and the percentage of ambiguous files means the proportion of ambiguous cloud-rain files in all cloud-rain files.

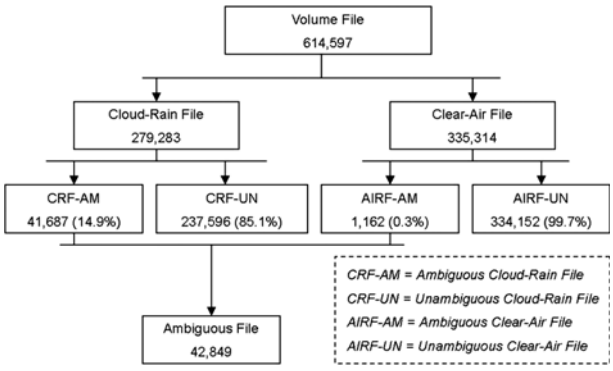

Fig. 2. Composition of the selected volume scan files. Dashed frames show the meanings of abbreviations.

a. Distribution of ambiguous files among stations and years

Figure 3 shows the percentages of ambiguous files in whole dataset. The yearly percentage of ambiguous files is the smallest in Fuzhou in 2009 (only 7.9%), and is the largest in Wenzhou in 2010, about 25.0%. The three-year average percentage of ambiguous files ranges from 11.1% to 20.5% among stations. From yearly perspective, large differences occur, because the yearly percentage of ambiguous files is the largest in 2010 and the smallest in 2009. From inter-station perspective, seashore radars (Fuzhou and Wenzhou) contain slightly more ambiguous files than inland radars (Hefei and Wuhan).

The velocity ambiguity depends on four factors: precipitation, wind speed, radar observation elevation angle, and maximum unambiguous velocity. Precipitation is the key factor. In ambiguous files, the year-to-year differences are due to year-to-year differences in precipitation, while the between-station differences are due to more typhoons and strong convections in coastal areas than in inland areas.

Thereby, numerous ambiguous data are present in each station in each year, so dealiasing of velocity fields is necessary for both seashore and inland radars.

b. Distribution of ambiguous files among types

In order to study the distribution of ambiguity among different types of echoes, the ambiguous files are divided into three types: stratus, weak convection, and strong convection.

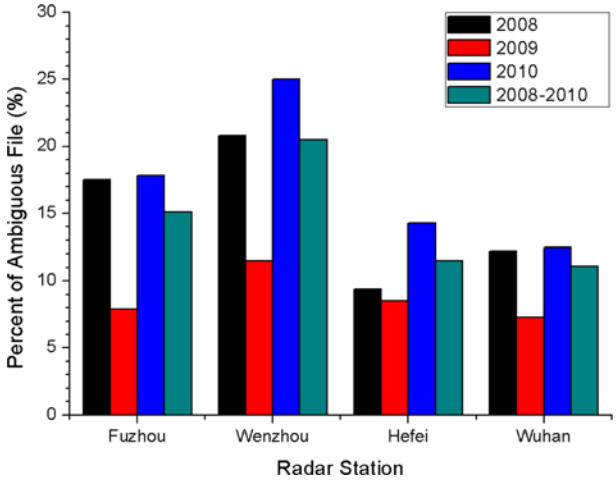

Fig. 3. Distribution of ambiguous files among stations and years.

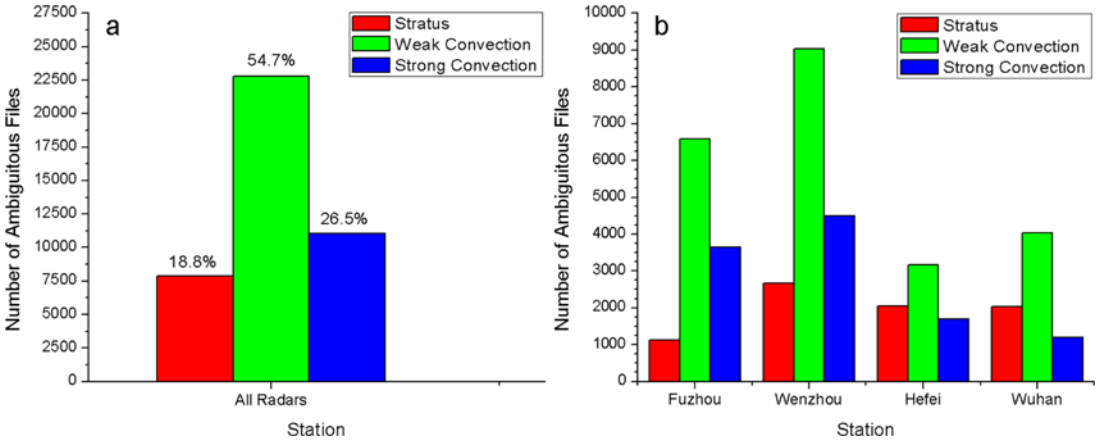

Fig. 4. Distribution of ambiguous files among types.

First, the 41,687 ambiguous files are divided manually by the echo shapes into stratus and convections. Then based on the maximum reflectivity factor Z_{max} after ground clutter suppression (Kessinger *et al*., 2001), the ambiguous convection files can be divided into two types. The files with $Z_{max} < 50$ *dBZ* are identified as weak convections; files with $Z_{max} \geq 50$ *dBZ* as strong convections. Two factors were considered for selection of this classification, one is the difficulty of dealiasing, and the other is the application of dealiasing algorithms. Generally, high reflectivity files can be easily dealiased as they contain few missing points, little noise, and have high continuity (Witt *et al*., 2009). But the opposite is true for low reflectivity files. This classification method can be easily combined with dealiasing algorithms, as it sets specific dealiasing thresholds for different types of ambiguous files, and thus improves the performance of dealiasing algorithms.

Figure 4a shows the distribution of ambiguous files among types. It can be seen that the number of ambiguous files is the highest in the type of weak convection (accounting for 54.7% of all ambiguous files), followed by strong convections (26.5%) and stratus (18.8%). Generally, strong convection data are prone to ambiguity, but strong convections usually occur in summer, but not very frequently. Weak convections occur frequently, especially in spring and fall, when the middle- and high-altitude strong winds will cause ambiguity in the weak convection data. Therefore, ambiguity is frequently seen in weak convection data. As shown in Fig. 4b, the number of weak convection files is the largest in all stations. Seashore radars (Fuzhou and Wenzhou) have more ambiguous strong-convection files than stratus ones, but inland radars (Hefei and Wuhan) have fewer ambiguous strong-convection files than stratus ones. This phenomenon occurs because the coastal areas are richer in vapors and more prone to strong convections such as typhoons, squall lines, or rainstorms.

Thereby, in designing and optimization of dealiasing algorithms for CINRAD-SA, more consideration should be given to weak convections and stratus. In algorithm validation, certain proportions of weak convections and stratus should be included.

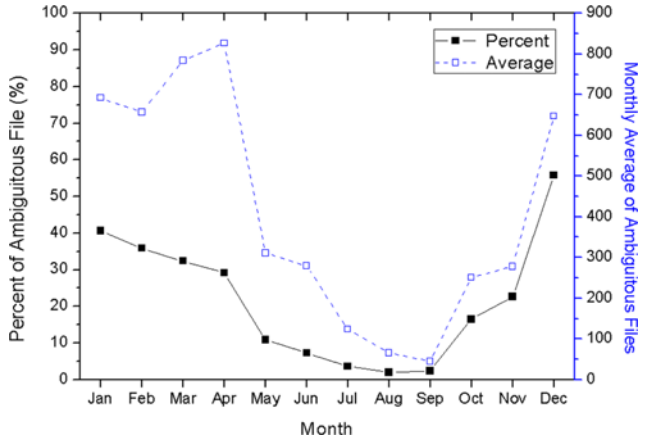

Fig. 5. Monthly distribution of ambiguous files.

c. Monthly distribution of ambiguous files

Figure 5 shows the monthly distribution of ambiguous files. It is clear that ambiguous files are present in any month. The percentage of ambiguous files first declines and then increases from January to December, and is the smallest in August (2.0%) and the largest in December (55.8%). Percentage of ambiguous files is larger than 30% from December to April next year, but is smaller than 10% from May to September. This phenomenon occurs because in winter and spring in China, the wind velocities at middle- and high-altitudes are very large and exceed the radar's Nyquist velocity, thereby causing ambiguity.

As the percentages and monthly averages of ambiguous files are small between July and September, interactive algorithms can be used for these three months. In other months, especially from December to April next year, only automatic algorithms can be used.

d. Distribution of ambiguous tilts with elevation angle

Each file contains 9 tilts, so in an ambiguous file, ambiguous points may not occur in all of the 9 tilts. Usually one or several

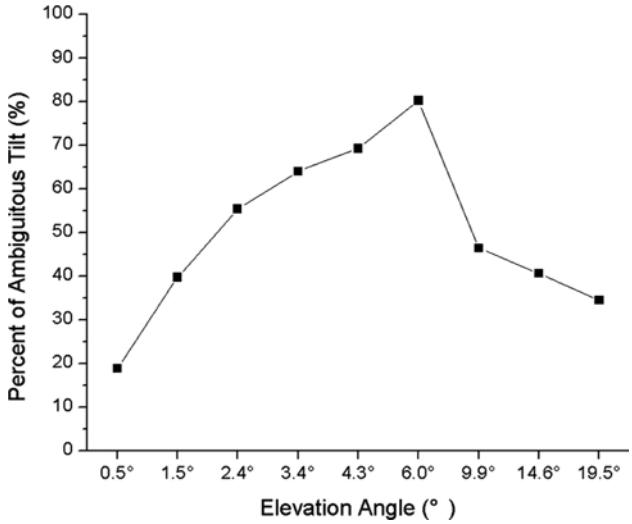

Fig. 6. Distribution of ambiguous tilts with elevation angle.

tilts are ambiguous, but the others are not. The statistics of ambiguous tilts in 41,687 ambiguous files is shown in Fig. 6. The number of ambiguous tilts first increases and then declines with the rise of elevation angle. Ambiguous tilts are the most at 6.0° (33,475), accounting for 80.3% of the total tilts at this angle. Ambiguous tilts are the fewest at 0.5° (7879), accounting for 18.9% of the total tilts at this angle. The second and third smallest percentages of ambiguous tilts are at 19.5° (34.5%) and 1.5° (39.7%), respectively.

This distribution can be explained as follows: at 0.5°, radars are detecting low-layer wind field, where wind speed is low and thus ambiguity rate is low. In general, wind velocity is increased with height. As elevation angle is gradually increased, the observation height also rises, so ambiguity rate is increased until it reaches the maximum at 6.0°. Above 6.0°, radars are detecting high-altitude wind close to the top of clouds. Here, the radars are detecting the radial component of wind, so with the increase of elevation angle, the radial component is decreased and thus ambiguity rate is reduced. Ambiguous tilts are distributed similarly for stratus, weak convections, and strong convections.

To reduce errors, the tilt with lowest ambiguity rate should be chosen for initialization of dealiasing algorithms. According to Fig. 6, if the interference from ground clutter is very small, the tilt 0.5° should be chosen as the initial tilt; otherwise, the 1.5° or 19.5° tilt can be chosen.

e. Distribution of ambiguous points with azimuth

The 41,687 ambiguous files contain 7.5×10^8 ambiguous points, whose azimuthal distribution is shown in Fig. 7. The ambiguous points (black) are azimuthally distributed as double peaks in symmetry around 150°. The two maxima occur near 70° and 250°; the two minima occur near 150° and 330°. The percentage of ambiguous points (blue) changes with azimuth in the same way as the number of ambiguous points. This

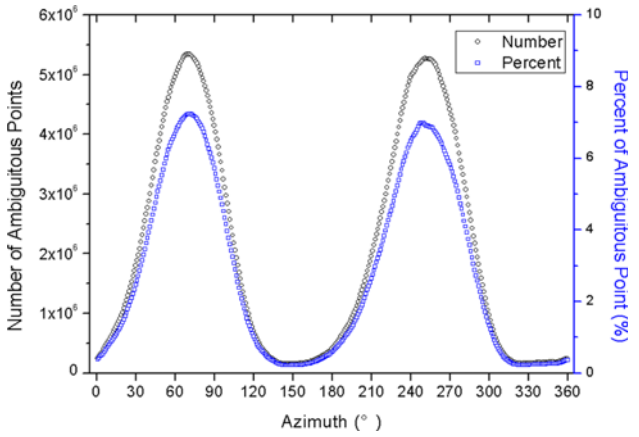

Fig. 7. Distribution of ambiguous points with azimuth.

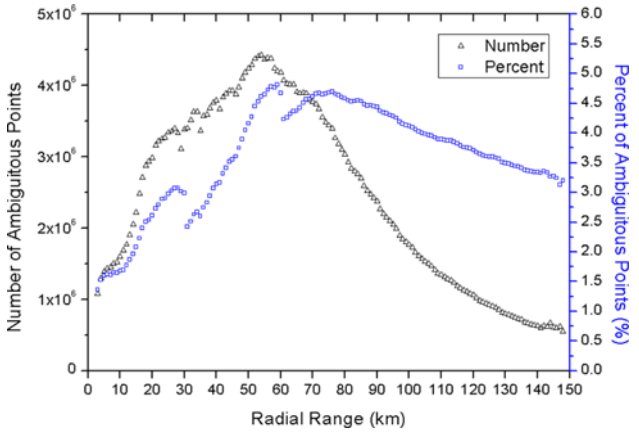

Fig. 8. Distribution of ambiguous points with radial range.

phenomenon is due to the prevailing wind in China. Radars detect the radial velocity of wind, so ambiguity most frequently occurs at the direction of prevailing wind.

Apparently, azimuth of 150° or 330°, which contains few ambiguous points, can be chosen as the initial radial direction for the dealiasing algorithms for CINRAD-SA.

f. Distribution of ambiguous points with radial distance

Figure 8 shows the radial distribution of ambiguous points. The number of ambiguous points (black) first increases and then decreases with distance, and reaches the maximum and minimum at 50-60 km and 140-150 km, respectively. The percentage of ambiguous points (blue) exceeds 3.0% when radial distance is larger than 50 km, and is smaller than 3.0% when radial distance is below 50 km, with the minimum of 1.3% near 0 km. In combination of the number distribution and the percentage distribution of ambiguous points, the area around 140-150 km shows a small number but a large percentage, so this area cannot be chosen as the initial radial point for dealiasing algorithms. When the impact of ground clutter is not considered, the number and the percentage of ambiguous points are both small at 0 km, so this area can be chosen as the

initial radial position. When the impact of ground clutter is considered, the radial initial points should be targeted at 30-40 km, where the impact is relatively small and thus ambiguity rate is low.

g. Distribution of ambiguous points with height

Figure 9 shows the distribution of ambiguous points with height. In Fig. 9, the number of ambiguous points (black) first increases and then decreases with height, and the maximum occurs at 5.5 km. When height is larger than 12 km, the number of ambiguous points is smaller than 10^6. The percentage of ambiguous points (blue) first increases and then decreases with height, and the maximum occurs at 6.5 km. When height is smaller than 3 km, the percentage of ambiguous points is smaller than 1.8%.

In order to improve performance, dealiasing algorithms such as the algorithm proposed by Gong *et al*. (2003) usually utilize VAD wind profiler as auxiliary reference. However, VAD can be severely affected by ambiguous points, so it has low accuracy at the height with a large number or percentage of ambiguous points. In Fig. 9, the number of ambiguous points is large at 4-7 km and the percentage of ambiguous points is large at 5-16 km, so at height 4-16 km, more preprocessing is needed before VAD retrieval to reduce the impact of ambiguous points.

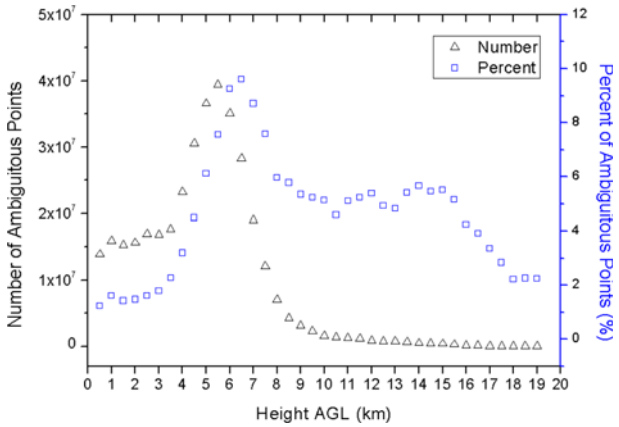

Fig. 9. Distribution of ambiguous point with height.

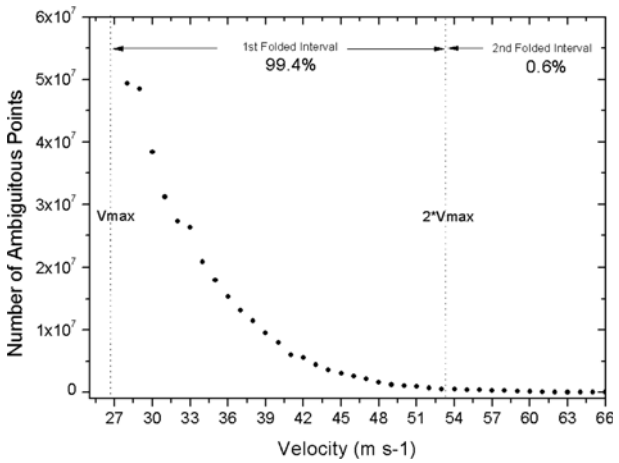

Fig. 10. Distribution of true velocity of ambiguous points.

h. Distribution of true velocities of ambiguous points

After 7.5×10^8 ambiguous points are recovered to true value V_T, the distribution of $|V_T|$ is shown in Fig. 10. When $|V_T|$ is near 27 m s^{-1}, the number of ambiguous points is the largest, but with the increase in $|V_T|$, the number is gradually reduced. About 99.4% of ambiguous points are located in 1st-folded interval, namely $|n| = 1$, but only 0.6% of ambiguous points are located in 2nd-folded interval, namely $|n| = 2$. Apparently, the ambiguity of CINRAD-SA is dominated by 1st-folded, so the dealiasing algorithms for CINRAD-SA should be targeted at solving 1st-folded ambiguity, and 2nd-folded ambiguity can be ignored. That is, in restoring the actual values of ambiguous data, n in Eq. (2) is restricted within (−1、0、+1). In this way, dealiasing time can be reduced, and once dealiasing errors occur, the wrong values will not deviate much from the real values.

4. Conclusions

Observations from CINRAD-SA operational radars were used to statistically analyzing the characteristics of velocity ambiguity, including occurrence rate, and inter-station, inter-type, temporal, and spatial distributions. The results show that: 1) Velocity ambiguity is common. About 14.9% of cloud-rain files and 0.3% of clear-air files are ambiguous. 2) With regard to the inter-station distribution, seashore radars contain more ambiguous files than inland radars; the yearly percentage of ambiguous files varies largely. 3) With regard to inter-type distribution, the number of ambiguous files is the largest in weak convections, about 57.9% of all ambiguous files. 4) With regard to monthly distribution, the number of ambiguous files is much larger in winter half year than summer half year, and ambiguity occurs frequently from December to April next year. 5) With regard to spatial distribution, ambiguous points most appear at the elevation angle of 6.0°, at the azimuths of 70° and 250°, at the radial distance of 50-60 km, and at the height of 5-6 km. 6) Most ambiguous points are 1st-folded, accounting for 99.4% of total ambiguous points.

The characteristics of velocity ambiguity can provide some reference for the design, optimization and validation of dealiasing algorithms. Based on the above conclusions, we provide the following suggestions on velocity dealiasing algorithms for CINRAD-SA. 1) Dealiasing of cloud-rain files is necessary for both seashore and inland radars. Automatic methods should be first considered, except for data from July to September, when interactive methods are more suitable. 2) The initial positions should be targeted at elevation angle of 1.5° or 19.5°, azimuth of 150° or 330°, and radial distance of 30-40 km. 3) When VAD retrieval is used as reference for dealiasing, more prepro-

cessing is needed for data at height of 4-16 km. 4) During validation, more attention should be given to ambiguous files of weak convections, to tilts with an elevation angle of 6.0°, and to ambiguous files between December and April next year.

Velocity ambiguity or dealiasing is very complex for weather radars and has been discussed since 1970s, but there are still many phenomena and relevant techniques that should be probed into. The conclusions in this paper only reveal the velocity ambiguity characteristics of CINRAD-SA. Based on these ambiguous characteristics, a great deal of work has to be done: validation of dealiasing effect on large-sample data; analysis of dealiasing effects on various echoes and different elevation angles; design of dealiasing approaches for various ambiguous data.

Acknowledgments. The work was supported by the National Natural Science Foundation of China (41375025), the China Special Fund for Meteorological scientific Research in the Public Interest (GYHY201106044), and A Project Funded by the Priority Academic Program Development of Jiangsu Higher Education Institutions (PAPD).

Edited by: Jong-Jin Baik

REFERENCES

Bargen, D. W., and R. C. Brown, 1980: Interactive radar velocity unfolding. Preprints. *19th Conf. on Radar Meteorology*, Miami, FL, Amer. Meteor. Soc., 278-283.

Bergen W. R., and S. C. Albers, 1988: Two- and three-dimensional dealiasing of Doppler radar velocities. *J. Atmos. Oceanic Technol.*, **5**, 305-319.

Boren, T. A., J. R. Cruz, and D. S. Zrnic, 1986: An artificial intelligence approach to Doppler weather radar velocity dealiasing. Preprints. *23rd Conf. on Radar Meteorology*, Snowmass, CO, Amer. Meteor. Soc., 107-110.

Browning, K. A., and R. Wexler, 1968: The determination of kinematic properties of a wind field using Doppler radar. *J. Appl. Meteorol.*, **7**, 105-113.

Doviak, R. D., and D. S. Zrnic, 1993: *Doppler Radar and Weather Observations.* 2nd ed. Academic Press, 562 pp.

Eilts, M. D., and S. D. Smith, 1990: Efficient dealiasing of Doppler velocities using local environment constraints. *J. Atmos. Oceanic Technol.*, **7**, 118-128.

Gao, J., and K. K. Droegemeier, 2004: A variational technique for dealiasing Doppler radial velocity data. *J. Appl. Meteorol.*, **43**, 934-940.

_____, L. Wang, and Q. Xu, 2003: A three-step dealiasing method for Doppler velocity data quality control. *J. Atmos. Oceanic Technol.*, **20**, 1738-1748.

Haase, G., and T. Landelius, 2004: Dealiasing of Doppler radar velocities using a torus mapping. *J. Atmos. Oceanic Technol.*, **21**, 1566-1573.

He, G., G. Li, X. Zou, and P. S. Ray, 2012: Applications of a velocity dealiasing scheme to data from the China new generation weather radar system (CINRAD). *Wea. Forecasting*, **27**, 218-230.

Hennington, L., 1981: Reducing the effects of Doppler radar ambiguities. *J. Appl. Meteorol.*, **20**, 1543-1546.

James, C. N., and R. A. Houze, 2001:A real-time four-dimensional Doppler dealiasing scheme. *J. Atmos. Oceanic Technol.*, **18**, 1674-1683.

Jing, Z., and G. Wiener, 1993: Two-dimensional dealiasing of Doppler velocities. *J. Atmos. Oceanic Technol.*, **10**, 798-808.

Kessinger, C., S. Ellis and J. VanAndel, 2001: NEXRAD data quality: The AP clutter mitigation scheme. Preprints. *30th Conf. on Radar Meteorology*, Munich, Germany, Amer. Meteor. Soc., 707-709.

Li, N., and M. Wei, 2010: An automated velocity dealiasing method based on searching for zero isodops. *Quart. J. Roy. Meteor. Soc.*, **136**, 1572-1582.

Merritt, M. W., 1984: Automatic velocity dealiasing for real-time applications. Preprints. *22nd Conf. on Radar Meteorology*, Zurich, Switzerland, Amer. Meteor. Soc., 528-533.

Ray, P. S., and C. Ziegler, 1977: Dealiasing first moment Doppler estimates. *J. Appl. Meteorol.*, **16**, 563-564.

Wei, M., Y. A. Liu, J. W. Pan, and N. Li, 2009: New velocity dealiasing of Doppler radar with the interactive method. Preprints. *World Congress on Computer Science and Information Engineering*, Los Angeles, CA, **5**, 7-11.

Witt, A., R. A. Brown, and Z. Jing, 2009: Performance of a new velocity dealiasing algorithm for the WSR-88D. Preprints. *34th Conf. on Radar Meteorology*, Williamsburg, VA, Amer. Meteor. Soc., P4.8.[Available online at http://ams.confex.com/ams/pdfpapers/155951.pdf.]

Xu, Q., K. Nai, L. Wei, P. Zhang, S. Liu, and D. Parrish, 2011: A VAD-based dealiasing method for radar velocity data quality control. *J. Atmos. Oceanic Technol.*, **28**, 50-62.

Yamada, Y., and M. Chong, 1999: VAD-based determination of the Nyquist internal number of Doppler velocity aliasing without wind information. *J. Meteor. Soc. Japan*, **77**, 447-457.

Zhang, J., and S. Wang, 2006: An automated 2D multipass Doppler radar volocity dealiasing scheme. *J. Atmos. Oceanic Technol.*, **23**, 1239-1248.